LARGE-GRAINED POLYCRYSTALLINE SILICON THIN-FILM SOLAR CELLS ON GLASS

S. Gall, K.Y. Lee, P. Dogan, B. Gorka, C. Becker, F. Fenske, B. Rau, E. Conrad, B. Rech
Hahn-Meitner-Institut Berlin
Kekuléstr. 5, D-12489 Berlin, Germany
Phone: +49-30-8062-1309, Fax: +49-30-8062-1333, E-mail: gall@hmi.de

ABSTRACT: Large-grained polycrystalline silicon (poly-Si) thin-film solar cells on glass were prepared using the 'seed layer concept' which is based on the homo-epitaxial thickening of large-grained poly-Si seed layers. Seed layers (p^+-type) were formed on glass by the aluminium-induced layer exchange (ALILE) process. Subsequently absorber layers (p-type) were grown homo-epitaxially onto the seed layer at temperatures of about 600°C using high-rate electron-beam evaporation. Post-deposition treatments (defect annealing and defect passivation) were used to improve the quality of the absorber layers. The pn-junctions were formed by the deposition of an n^+-type a-Si:H emitter. Finally transparent conductive oxides (ZnO:Al) were deposited and solar cells were processed. The best solar cell obtained so far showed an active area efficiency of 2.7%. In addition to our standard process we studied also the implementation of advanced concepts, namely the seed layer formation on nano-textured glass and on ZnO:Al coated glass.
Keywords: Polycrystalline, Silicon, Thin Film

1 INTRODUCTION

So far the existing silicon thin-film solar cells on glass which are based on amorphous silicon (a-Si:H) or microcrystalline silicon (μc-Si:H) are limited to single junction efficiencies of about 10%. To overcome the current limits new approaches are necessary. This paper deals with such a new approach which could lead to higher material quality and consequently to higher efficiencies. The approach is based on the preparation of large-grained polycrystalline silicon (poly-Si) films on glass using the 'seed layer concept': In a first step a very thin large-grained poly-Si film (seed layer) is formed on the glass substrate and in a second step this seed layer is homo-epitaxially thickened to form the absorber layer (base) of the solar cell. In this paper we describe the current status of the development of such large-grained poly-Si thin-film solar cells at the Hahn-Meitner-Institut Berlin.

The schematic structure of the poly-Si thin-film solar cells under investigation is shown in Fig. 1. It consists of a p^+-type poly-Si seed layer, a p-type poly-Si absorber, an n^+-type a-Si:H emitter, a transparent conductive oxide (TCO), and metal contacts to both TCO and absorber (not shown here). Figure 2 shows the sequence of process steps used for the preparation of the poly-Si thin-film solar cells schematically shown in Fig. 1. After the formation of a large-grained poly-Si seed layer on the glass substrate the absorber of the solar cell is grown homo-epitaxially. Then two post-deposition treatments (defect annealing followed by defect passivation) are applied to improve the quality of the poly-Si layers. To form the pn-junction a low-temperature a-Si:H emitter is deposited. Finally the contacts (TCO and metal grids) are formed. In the following section the different process steps are described in detail. In addition to our standard processes we discuss also the implementation of advanced concepts which could lead to improved solar cell properties in the future.

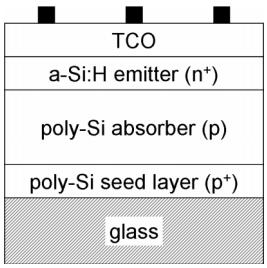

Figure 1: Schematic structure of a poly-Si thin-film solar cell on glass consisting of a p^+-type poly-Si seed layer, a p-type poly-Si absorber, an n^+-type a-Si:H emitter, a transparent conductive oxide (TCO), and metal contacts to both TCO and absorber (not shown here).

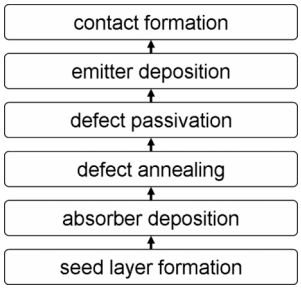

Figure 2: Sequence of process steps for the preparation of poly-Si thin-film solar cells on glass.

2 SOLAR CELL PREPARATION

2.1 Seed layer formation

Large-grained poly-Si seed layers were formed directly on cleaned glass substrates (Borofloat 33 from Schott) using the aluminium-induced layer exchange (ALILE) process which is based on aluminium-induced crystallisation (AIC) of amorphous silicon (a-Si) [1-3]. The glass substrates were cleaned using a glass cleaning solution (Mucasol). Starting point for the ALILE process is the following stack: glass/Al(300nm)/a-Si(375nm). Both layers (Al and a-Si) were deposited in the same chamber by DC magnetron sputtering. The ALILE

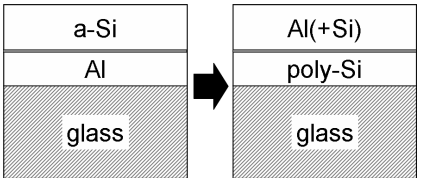

Figure 3: Schematic illustration of the aluminium-induced layer exchange (ALILE) process. During an annealing step the initial glass/Al/a-Si stack is transformed into a glass/poly-Si/Al(+Si) stack. The permeable membrane between the layers (grey line) stays in place during the ALILE process.

process requires a thin permeable membrane between the Al and the a-Si layer which controls the diffusion of Al and Si. The membrane (a thin Al oxide layer) was formed by exposure to air of the Al-coated glass substrate (prior to the a-Si deposition). Annealing of the initial glass/Al/a-Si stack at temperatures below the eutectic temperature of the Al/Si system (T_{eu} = 577°C) leads to a layer exchange and a concurrent crystallisation of Si. Our standard annealing temperature is 450°C. Details about the nucleation and the subsequent grain growth during the ALILE process can be found in [4-6]. At the end of the process a glass/poly-Si/Al(+Si) stack is formed (Fig. 3). The membrane stays in place during the entire ALILE process. Thus, the thickness of the resulting poly-Si film is determined by the thickness of the initial Al layer (300nm). The layer on top of the poly-Si film consists of Al and some Si inclusions ('Si islands'). Finally the Al(+Si) layer and the membrane were removed by chemical mechanical polishing (CMP). The resulting thickness of the poly-Si seed layer is about 200nm.

The seed layers prepared with the ALILE process are heavily doped (p^+-type) with Al which is an acceptor in Si. Therefore the seed layers act as a Back Surface Field (BSF) in our solar cell structure. Characteristic features of the seed layer are a large grain size and a preferential (100) orientation of the grain surface. The preferential (100) orientation of the seed layer is favourable for the subsequent homo-epitaxial growth of the absorber at temperatures compatible with the glass substrate (up to about 600°C). For example, a seed layer prepared at 425°C showed an average grain size of 7µm, a maximum grain size of 18µm, and a preferential (100) orientation $R_{(100)}$ of about 60% [7-9] ($R_{(100)}$ is defined as the percentage of the seed layer surface which is tilted by less than 20° with respect to the perfect (100) orientation). Preferential (100) orientations $R_{(100)}$ of up to 75% were obtained [10].

Light-trapping, which plays a key role for crystalline Si thin-film solar cells, is not yet implemented in our standard solar cell structure (see Fig. 1). The application of textured glass substrates instead of planar glass substrates is an attractive way to implement light-trapping (especially for the superstrate configuration where the light enters the solar cell through the glass). In collaboration with Saint Gobain Recherche (SGR) we carried out seed layer formation experiments on textured glass. Applying a special plasma etching process [11-12], SGR prepared nano-textured glass substrates with different roughness (using Borofloat 33 from Schott). We used these nano-textured glass substrates for the ALILE process. Continuous poly-Si seed layers were formed on the nano-textured glass, too. Compared to seed layers on un-textured glass the grain size is slightly decreased, but still larger than 5µm [8] (the grain size of seed layers on nano-textured glass was estimated using an optical microscope). The nano-textured glass surface is still present under the seed layer. The results obtained so far are quite promising. However, the removal of the Al(+Si) layer and the membrane using CMP remains a big challenge. The maximum roughness of the nano-textured glass is strongly limited by the CMP process (if the roughness is too high, the seed layer is partially polished off). Thus, an alternative technique to remove the top layers is required to use nano-textured glass in a standard process. A successful implementation of nano-textured glass would improve the poly-Si thin-film solar cells significantly.

Although the poly-Si seed layer is highly doped with Al the sheet resistance is too high for high-efficiency solar cells. An appealing option to reduce the sheet resistance is the application of TCO-coated glass as substrate for the ALILE process. In our experiments we used smooth ZnO:Al films which were deposited at the 'Forschungszentrum Jülich' (FZJ) on cleaned glass substrates (Borofloat 33 from Schott) using non-reactive RF sputtering from a ceramic target. Also the ALILE process on ZnO:Al-coated glass leads to continuous poly-Si seed layers. After removal of the Al(+Si) layer and the membrane (using CMP) the structural properties of the seed layer were investigated at IMEC by Electron Back Scatter Diffraction (EBSD) [7-9]: A seed layer prepared at 425°C showed an average grain size of 5µm and a maximum grain size of 16µm. This means that the grain size on ZnO:Al-coated glass is slightly smaller than on bare glass. The grain size of seed layers on ZnO:Al-coated glass decreases with increasing annealing temperature (as on bare glass). The preferential (100) orientation $R_{(100)}$ of the seed layer formed at 425°C was about 60% which means that $R_{(100)}$ is not affected by the ZnO:Al layer underneath. So far the results on ZnO:Al-coated glass are quite encouraging. The successful application of ZnO:Al-coated glass for poly-Si thin-film solar cells would lead to lower series resistances and consequently to higher efficiencies. A ZnO:Al layer between glass and seed layer is attractive for poly-Si thin-film solar cells in both configurations: substrate and superstrate. The successful application of textured ZnO:Al films instead of smooth ZnO:Al films would not only lead to lower series resistances but also to enhanced light-trapping.

2.2 Absorber deposition

The p-type absorber layers were grown homo-epitaxially onto cleaned substrates by electron-beam evaporation of silicon (for our experiments FZ material was used). No additional ionisation stage was used. The standard thickness of the grown films is about 2µm. Doping was obtained by co-evaporation of boron using a high-temperature effusion cell. The resulting boron concentration is about $5x10^{16}cm^{-3}$ (determined by Secondary Ion Mass Spectrometry - SIMS). As substrates both poly-Si seed layers on glass and monocrystalline Si wafers ('ideal seed layers') were used. The substrates were cleaned by a standard RCA procedure and a final HF-dip (directly before the samples were loaded into the

vacuum chamber). Due to the application of glass substrates the process temperature is limited to about 600°C. This temperature limit is very crucial for the epitaxial growth because Si epitaxy usually takes place at much higher temperatures (above 1000°C). Electron-beam evaporation is a very attractive technique for the absorber deposition because (i) high deposition rates (up to about 1µm/min) can be used, (ii) no UHV conditions are required, (iii) no toxic gases are used, and it is up-scalable to large areas for industrial production. For our experiments the base pressure was about $1x10^{-8}$mbar and the residual gas pressure during deposition was about $1x10^{-6}$mbar.

We investigated the influence of both deposition temperature (450…700°C) and deposition rate (40…475nm/min) on the properties of the grown films. In order to analyse the structural quality of the grown films Secco-etching was applied to the films grown on Si(111) wafers. Scanning electron microscopy (SEM) investigations of these films showed that (i) the higher the deposition temperature the lower is the number of extended defects and (ii) the higher the deposition rate the higher is the number of extended defects [13]. It is known that the structural quality of homo-epitaxial grown films strongly depends on the crystallographic orientation of the underlying substrate. Films grown on Si(100) wafers feature the best structural quality (compared to films on Si(110) and Si(111) wafers) [14]. The advantage of (100) surfaces for the subsequent homo-epitaxial growth was also observed on films grown on poly-Si seed layers on glass [13]. This confirms the importance of a high preferential (100) orientation of the seed layer grains. The films grown on seed layers feature a very high aluminium concentration of 10^{17}cm^{-3} or even more (determined by SIMS) [15]. This is by far too high. Further investigations are needed to clarify the origin.

2.3 Defect annealing

An attractive way to improve the quality of grown Si films is the application of a post-deposition defect annealing step (i.e. a short high temperature treatment). We carried out the defect annealing in nitrogen atmosphere using a Rapid Thermal Annealing (RTA) system. It was shown that the applied temperature profile should be adapted to the properties of the glass [16]. We also used an adapted temperature profile for our defect annealing: The temperature region between the strain point (518°C) and the annealing point (560°C) of Borofloat 33 from Schott was passed with moderate heating and cooling rates [15]. In our experiments we varied both annealing temperature (i.e. maximum temperature) and annealing time (i.e. duration of the treatment at the maximum temperature). Annealing temperatures between 800°C and 1000°C were applied for 5 to 300 seconds. To investigate the influence of the different RTA treatments solar cell test structures were prepared (no defect passivation was applied). So far, the best results were obtained at an annealing temperature of 950°C and an annealing time of 200 seconds: The open circuit voltages of the solar cell test structures were more than doubled to about 290mV [15]. This shows the importance of such a treatment for the development of efficient poly-Si thin-film solar cells. Finding a suitable combination of annealing time and annealing temperature plays a key role for the optimisation of this process.

2.4 Defect passivation

It is well known that hydrogen is capable to passivate defects in Si. But due to the deposition techniques and the temperatures applied during the previous process steps the hydrogen concentration in the films is rather low. Therefore an additional post-deposition hydrogen treatment is necessary to passivate defects in the grown Si films. The importance of hydrogen passivation for poly-Si thin-film solar cells was impressively shown by CSG Solar for films prepared by solid phase crystallisation (SPC) [17]. They used temperatures of about 600°C to get efficient passivation. We carried out hydrogenation experiments in a special plasma tool which allows for substrate temperatures of up to 650°C. The remote lamp heater enables rapid heating and cooling. Like in the case of defect annealing a moderate heating rate is applied. When the passivation temperature is reached the hydrogen plasma is ignited. After the passivation time the sample is cooled down rapidly to 350°C. This takes about 3 minutes. During that time the hydrogen plasma remains ignited. This prevents out-diffusion of hydrogen. The influence of the defect passivation was studied again by solar cell test structures. For these experiments no defect annealing was applied. Using a passivation temperature of 620°C and a passivation time of 10 minutes open circuit voltages of about 390mV were obtained [18]. It is expected that an optimisation of the defect passivation will lead to further improvements.

2.5 Emitter deposition

The n^+-type a-Si:H emitter was deposited onto the p-type absorber layer by plasma enhanced chemical vapour deposition (PECVD). The a-Si:H layer was grown at 200°C (low-temperature emitter) and the film thickness was about 10nm. The deposition parameters were identical to ones which had led to high-efficiency wafer-based a-Si:H/c-Si heterojunction solar cells [19]. So far no special optimisation for poly-Si thin-film solar cells has taken place.

2.6 Contact formation

On top of the n^+-type a-Si:H emitter a transparent conductive oxide (ZnO:Al) was deposited by reactive DC magnetron sputtering (film thickness was about 80nm). The emitter areas were defined by photolithography and subsequent wet-chemical mesa etching. After mesa etching metal (Al) contacts were formed on both the TCO and the absorber. The shape of the metal contacts was also defined by photolithography (using a lift off process). Solar cells with two different total areas were prepared (1cm x 1cm and 4mm x 4mm).

3 SOLAR CELL RESULTS

The dark current-voltage characteristic of the best solar cell obtained so far is shown in Fig. 4. This solar cell has interdigitated contacts. The total area of this solar cell is 16mm^2. The dark current density was calculated using the emitter area of the solar cell (8.55mm^2). The forward bias behaviour was fitted with a two-diode model. The diode which describes the diffusion current (with an ideality factor of one) is dominating. The corresponding saturation current density is about $1.7x10^{-4}$mA/cm^2. The diode which describes the

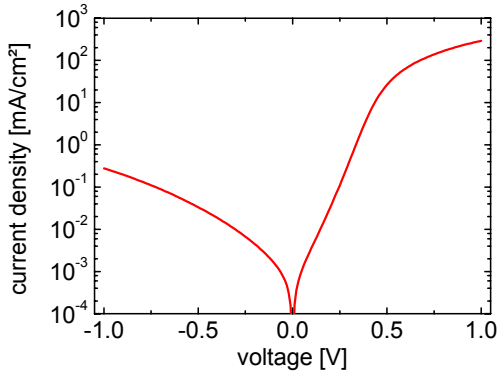

Figure 4: Dark current-voltage characteristic of the best solar cell. The current density was calculated using the emitter area.

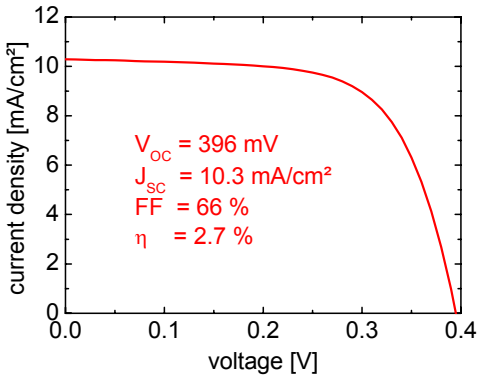

Figure 5: Current-voltage characteristic of the best solar cell under illumination (AM1.5, 100mW/cm2, 25°C). The current density and the efficiency were calculated using the active area.

recombination current in the space charge region (with an ideality factor of two) can almost be neglected. The corresponding saturation current density is about 7.0×10^{-4} mA/cm^2 (or less if a lower shunt resistance is taken into account). The current-voltage characteristic of this solar cell under illumination (AM1.5, 100mW/cm^2, 25°C) is shown in Fig. 5. Here, the current density was calculated using the active area of the solar cell: 7.44mm^2 (emitter area minus emitter contact area). For the measurement white paper was placed below the glass substrate. This led to an increase of the short circuit current density J_{sc} from 8.1mA/cm^2 (black reflector) to 10.3mA/cm^2 (white reflector). Together with an open circuit voltage V_{oc} of 396mV and a fill factor FF of 66% this has led to an active area efficiency of 2.7%.

4 SUMMARY AND CONCLUSIONS

Thin large-grained poly-Si films were prepared on glass using the 'seed layer concept'. The seed layers prepared by the ALILE process were thickened homo-epitaxially using electron-beam evaporation. Post-deposition treatments (defect annealing and defect passivation) were applied to improve the material quality. Using this material poly-Si thin-film solar cells were processed. The best solar cell we obtained so far showed an active area efficiency of 2.7% (V_{oc} = 396mV, J_{sc} = 10.3mA/cm^2, FF = 66%).

Our V_{oc} and J_{sc} results are somewhat lower than results recently published for a similar cell concept (epitaxial thickening of an ALILE seed layer using ion-assisted deposition) [20]. With a high temperatures approach (above 1000°C), efficiencies of up to 8% were already obtained [21]. This shows that the potential of the cell concept under investigation is far above the results we obtained so far. To reach efficiencies of 10% and more the material quality has to be improved dramatically. Therefore, contamination levels and intra-grain defect densities have to be reduced significantly. Furthermore, also the device structure has to be improved by the application of suitable light-trapping and contacting schemes. In first experiments the implementation of such advanced concepts, namely the seed layer formation on nano-textured glass and on ZnO:Al coated glass, showed promising results.

5 ACKNOWLEDGEMENTS

The authors would like to thank (i) D. Le Bellac from Saint Gobain Recherche, France for the preparation of nano-textured glass substrates, (ii) I. Gordon and J. D'Haen from IMEC, Belgium for the EBSD in-vestigations of the seed layers and last but not least (iii) S. Common, K. Jacob, C. Klimm, M. Muske, and T. Weber from HMI for their assistance during sample preparation.

This work has been financially supported by the European Commission in the framework of the FP6 project 'Advanced Thin-Film Technologies for Cost Effective Photovoltaics' (ATHLET) [contract number: 019670].

6 REFERENCES

[1] O. Nast, T. Puzzer, L.M. Koschier, A.B. Sproul, S.R. Wenham, Applied Physics Letters 73 (1998) 3214.

[2] O. Nast, S.R. Wenham, Journal of Applied Physics 88 (2000) 124.

[3] O. Nast, A.J. Hartmann, Journal of Applied Physics 88 (2000) 716.

[4] J. Schneider, J. Klein, M. Muske, S. Gall, W. Fuhs, Applied Physics Letters 87 (2005) 031905-1.

[5] J. Schneider, J. Klein, A. Sarikov, M. Muske, S. Gall, W. Fuhs, Materials Research Society Symposium Proceedings 862 (2005) A2.2.1.

[6] J. Schneider, A. Schneider, A. Sarikov, J. Klein, M. Muske, S. Gall, W. Fuhs, Journal of Non-Crystalline Solids 352 (2006) 972.

[7] K.Y. Lee, M. Muske, I. Gordon, M. Berginski, J. D'Haen, J. Hüpkes, S. Gall, B. Rech, submitted to Thin Solid Films (E-MRS Spring Meeting 2007).

[8] K.Y. Lee, C. Becker, M. Muske, S. Gall, B. Rech, I. Gordon, J. D'Haen, M. Berginski, J. Hüpkes, Proc. 22nd European Photovoltaic Solar Energy

Conference, Milan, Italy (2007) – this conference.
[9] I. Gordon, D. Van Gestel, L. Carnel, G. Beaucarne, J. Poortmans, K.Y. Lee, P. Dogan, B. Gorka, C. Becker, F. Fenske, B. Rau, S. Gall, B. Rech, J. Plentz, F. Falk, D. Le Bellac, Proc. 22nd European Photovoltaic Solar Energy Conference, Milan, Italy (2007) – this conference.
[10] S. Gall, J. Schneider, J. Klein, K. Hübener, M. Muske, B. Rau, E. Conrad, I. Sieber, K. Petter, K. Lips, M. Stöger-Pollach, P. Schattschneider, W. Fuhs, Thin Solid Films 511-512 (2006) 7.
[11] N.-P. Harder, D. Le Bellac, E. Royer, B. Rech, G. Schöpe, J. Müller, Proc. 19th European Photovoltaic Solar Energy Conference, Paris, France (2004) 1355.
[12] C. Gandon, C. Marzolin, B. Rogier, E. Royer, Patent WO 02/02472 A1 (2002).
[13] P. Dogan, F. Fenske, L.-P. Scheller, K.Y. Lee, B. Gorka, B. Rau, E. Conrad, S. Gall, B. Rech, Proc. 22nd European Photovoltaic Solar Energy Conference, Milan, Italy (2007) – this conference.
[14] B. Gorka, P. Dogan, I. Sieber, F. Fenske, S. Gall, Thin Solid Films 515 (2007) 7643.
[15] B. Rau, K.Y. Lee, P. Dogan, F. Fenske, E. Conrad, S. Gall, Proc. 22nd European Photovoltaic Solar Energy Conference, Milan, Italy (2007) – this conference.
[16] M.L. Terry, A. Straub, D. Inns, D. Song, A.G. Aberle, Proc. 31st IEEE Photovoltaic Specialists Conference, Lake Buena Vista, USA (2005) 971.
[17] M.J. Keevers, A. Turner, U. Schubert, P.A. Basore, M.A. Green, Proc. 20th European Photovoltaic Solar Energy Conference, Barcelona, Spain (2005) 1305.
[18] B. Gorka, B. Rau, K.Y. Lee, P. Dogan, F. Fenske, E. Conrad, S. Gall, B. Rech, Proc. 22nd European Photovoltaic Solar Energy Conference, Milan, Italy (2007) – this conference.
[19] E. Conrad, K. v. Maydell, H. Angermann, C. Schubert, M. Schmidt, Proc. 4th World Conference on Photovoltaic Energy Conversion, Waikoloa, USA (2006) 1263.
[20] A.G. Aberle, Journal of Crystal Growth 287 (2006) 386.
[21] I. Gordon, L. Carnel, D. Van Gestel, G. Beaucarne, J. Poortmans, Progress in Photovoltaics (2007) accepted (DOI: 10.1002/pip.765)